Towards water-free tellurite glass fiber for 2-5 μm nonlinear applications

Xian Feng, Jindan Shi, Martha Segura, Nicolas M. White, Pradeesh Kannan, Laurent Calvez, Xianghua Zhang, Laurent Brilland, Wei H. Loh

Fibers **2013**, *1*, 70-81; doi:10.3390/fib1030070

OPEN ACCESS

fibers

ISSN 2079-6439

www.mdpi.com/journal/fibers

Article

Towards Water-Free Tellurite Glass Fiber for 2–5 µm Nonlinear Applications

Xian Feng [1,*], Jindan Shi [1], Martha Segura [1], Nicolas M. White [1], Pradeesh Kannan [1], Laurent Calvez [2], Xianghua Zhang [2], Laurent Brilland [3] and Wei H. Loh [1]

[1] Optoelectronics Research Centre, University of Southampton, Southampton, SO17 1BJ, UK; E-Mails: jxs@orc.soton.ac.uk (J.S.); m.segura-sarmiento@soton.ac.uk (M.S.); nmw@orc.soton.ac.uk (N.M.W.); pk2e10@orc.soton.ac.uk (P.K.); whl@orc.soton.ac.uk (W.H.L.)

[2] Laboratory of Glasses and Ceramics, University of Rennes I, UMR CNRS 6226, Rennes Cedex 35042, France; E-Mails: laurent.calvez@univ-rennes1.fr (L.C.); xiang-hua.zhang@univ-rennes1.fr (X.Z.)

[3] PERFOS; R&D platform of Photonics Bretagne, 11 rue Louis de Broglie, Lannion 22300, France; E-Mail: laurent.brilland@univ-rennes1.fr

***** Author to whom correspondence should be addressed; E-Mail: xif@orc.soton.ac.uk; Tel.: +44-023-8059-9104; Fax: +44-023-8059-3149.

Received: 22 October 2013; in revised form: 13 November 2013 / Accepted: 14 November 2013 / Published: 22 November 2013

Abstract: We report our recent progress on fabricating dehydrated tellurite glass fibers. Low OH content (1 ppm in weight) has been achieved in a new halogen-containing lead tellurite glass fiber. Low OH-induced attenuation of 10 dB/m has been confirmed in the range of 3–4 µm using three measurement methods. This shows the dehydrated halo-tellurite glass fiber is a promising candidate for nonlinear applications in a 2–5 µm region.

Keywords: glass fiber materials; nonlinear optical fibers; mid-infrared

---

1. Introduction

The mid-infrared (mid-IR) 2–5 µm region is one of the atmospheric transmission windows, where the Earth's atmosphere is relatively transparent. It is an important area for use of remote laser sensing for atmospheric, security and industrial applications, such as detecting remote explosives,

countermeasures against heat-seeking missiles and covert communication systems [1]. A 2–5 μm broadband or tunable laser source with a medium or high average power level (100 mW–10 W) is therefore in high demand. To realize this purpose, typically $\chi^{(2)}$ nonlinear crystal based optical parametric oscillators (OPOs) are used. However, with such an output power level and wide wavelength tunability, the size of crystal OPO is normally large and requires complicated optical configurations. Instead, recent progress in dispersion tailored highly nonlinear microstructured optical fibers [2] has shown that fiber-based $\chi^{(3)}$ nonlinear laser sources, such as the supercontinuum [3], fiber OPO [4], or frequency comb [5] can also fulfill this task. What is more, fiber lasers show significant advantages over other solid state lasers as an effective approach to provide economic, compact and flexible optical components. Also excellent beam quality can be given from a single mode fiber.

A 2–5 μm mid-IR fiber nonlinear laser source should be based on a fiber using a nonlinear glass with high transparence in 2–5 μm. The position of the IR absorption edge, *i.e.*, the infrared longwave transmission limit, of an optical glass is intrinsically limited by the multiphonon absorption edge of the glass. This can be simply explained by Hooke's law using the two-mass spring model [6]. In general, as summarized in Table 1, non-silica glasses, such as tellurite (TeO_2 based), fluoride (typically ZrF_4 or AlF_3 based), and chalcogenide (chalcogen S, Se, Te based) glasses [7–9], possess excellent optical transparence in the wavelength range of 0.4–7 μm, 0.3–8 μm and 1–16 μm respectively, and thus are promising candidates as fiber materials for mid-infrared nonlinear optical applications over the conventional silica glass. The latter shows inferior transparence beyond 2 μm, due to (i) the strong fundamental vibration hydroxyl absorption at 2.7 μm, and (ii) high loss (>50 dB/m) starting from 3 μm due to the tail of the multi-phonon absorption of Si-O network.

Table 1. Comparison of various optical glasses as host materials for mid-infrared nonlinear fibers [7–9].

	Silica (SiO_2 based)	**Tellurite (TeO_2 based)**	**Fluoride (ZrF_4 or AlF_3 based)**	**Chalcogenide (chalcogen S, Se, Te based)**
Refractive index n at 1.55 μm	1.46	2–2.2	1.5–1.6	2.3–3
Nonlinear refractive index n_2 ($\times 10^{-20}$ m^2/W)	2.5	20–50	2–3	100–1000
λ_0, zero dispersion wavelength of material (μm)	~1.3	~2	~1.7	>5
IR longwave transmission limit	up to 3 μm	6–7 μm	7–8 μm	12–16 μm
Thermal stability for fiber drawing	excellent	good	poor	good
Viscosity around fiber drawing temperature	flat	steep	steep	flat
Durability in environment	excellent	good	poor, hygroscopic	good
Toxicity	safe	safe	relatively high	relatively high

Technically, tellurite glasses can be regarded as a high-index, highly nonlinear version of fluoride glasses. First, their viscosity curves in the range of the fiber drawing temperatures are both relatively steep [10]. Second, both tellurite and fluoride glasses have the zero dispersion wavelength of the bulk

material at ~2 µm [11]. Also the longwave transmission limits of these two glass types are both located at ~ 6–7 µm. But tellurite glasses have high refractive index n (2.0–2.2) and nonlinear refractive index n_2 (20–50 × 10^{-20} m^2/W), while fluoride glasses typically have n of ~1.5 and n_2 of ~2 × 10^{-20} m^2/W. From Table 1, it is seen that chalcogenide glasses show excellent IR transmission up to 16 µm and possesses high n_2 of 100–1000 × 10^{-20} m^2/W. However, its zero dispersion wavelength of the bulk is beyond 5 µm. In order to make a chalcogenide glass nonlinear fiber with a zero dispersion wavelength close to 1.5 or 2 µm, which is the lasing wavelength of the conventional erbium or thulium doped fiber lasers, very large waveguide dispersions need to be introduced, requiring the final fiber core diameter to be submicron. This is disadvantageous for power scaling. Therefore, tellurite glasses are an ideal host material as a fiber nonlinear medium for 2–5 µm wavelength range. In principle, broadband mid-IR four-wave-mixing can be realized using a single mode large mode area tellurite fiber pumped with a high power Tm/Ho doped fiber laser [12].

Figure 1. Comparison of absorption coefficients of some selected impurities in a conventional tellurite glass (composition: 75TeO_2-20ZnO-5Na_2O, mol.%) (summarized from results in Reference [13].)

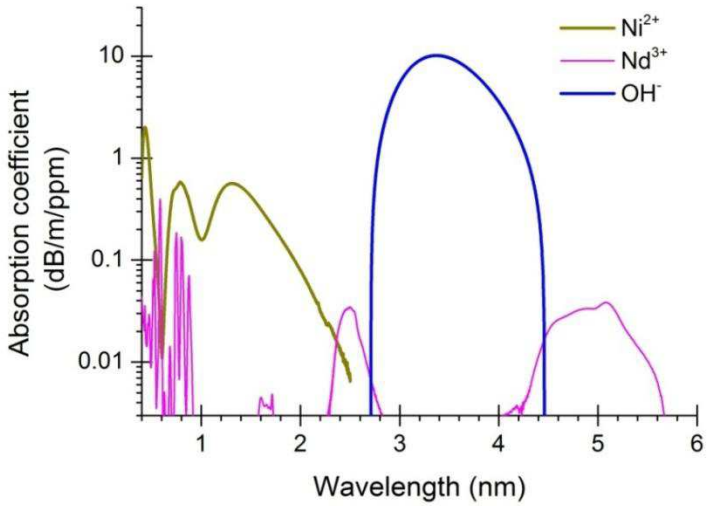

Water, commonly existing in many optical materials as the hydroxyl group OH^-, is usually difficult to be eliminated. The absorption spectrum of the OH fundamental vibration is around 3 µm and varies with the glass composition. In pure silica, the fundamental vibration of OH band is located at 2.70 (± 0.02) µm and with an extinction coefficient of 10 dB/m/ppm (in weight) [14], while in ZrF_4-based fluoride glass, it is located at 2.87 µm with an extinction coefficient of 5 dB/m/ppm (in weight) [15]. For tellurite glass, the fundamental vibration of OH band has an extinction coefficient of ~1 dB/m/ppm (in mole) or ~10 dB/m/ppm (in weight) [16], but it is much wider than the above two glasses and ranges from 3–4 µm. This is because the wavelength of the fundamental OH vibration reflects the strength of OH bonding with the surrounding molecules. The large variety of deformed [TeO_4] and [TeO_3] units in tellurite glass network causes very different sites of OH groups and consequently the bond strength of OH groups shows much larger variation [16]. This is very different from the situation of pure silica glass, in which the [SiO_4] tetrahedra units are identical in the short range leading to the fundamental OH absorption as narrow as ~150 nm (~200 cm^{-1}) [15]. Based on the data given in Ref. [13], Figure 1

shows the measured transmission spectra of bulk tellurite glasses (base: $75TeO_2$-$20ZnO$-$5Na_2O$, mol.%) doped with the impurities including the transition metal (TM) ion Ni^{2+}, the rare earth (RE) ion Nd^{3+}, and the hydroxyl group OH^-. It is seen that the fundamental vibration of the hydroxyl group OH^- is the most harmful impurities for blocking the transmission of a tellurite glass in 2–5 μm region, in terms of the wide absorption range (3–4 μm) and the high peak absorption coefficient (10 dB/m/ppm). Because the nonlinearity n_2 of tellurite glasses is one order of magnitude higher than those of silica and fluoride glasses, less than a meter length of tellurite nonlinear fiber is acceptable for many nonlinear optical applications, indicating that an acceptable OH peak absorption loss is no more than the level of 10 dB/m. In other words, the OH impurity in a usable tellurite glass fiber should be no more than the level of 1 ppm in weight. It must be pointed out that, without any dehydration process, the tellurite glass, which was prepared in the open atmosphere, has a strong water absorption coefficient of ~1400 dB/m peaking at 3.4 μm [16]. Therefore, even an 8 mm-long non-dehydrated tellurite glass fiber, will suffer a 15–20 dB loss in the range of 3–4 μm [17]. Since the tail of multiphonon absorption of tellurite glasses starts from ~5 μm, a proper dehydration process is the key to extend the high transmission window (*i.e.*, absorption coefficient < 0.1 cm^{-1}) of a tellurite glass fiber to 5 μm.

In this work, we have prepared the tellurite glass preforms in an ultradry atmosphere filled glovebox, and halide compounds are added into the tellurite glass compositions. The fabricated dehydrated halo-tellurite glass fibers show low OH induced attenuation from 3–4 μm, indicating that they are promising candidates for 2–5 μm nonlinear optical applications.

2. Experimental Section

An ultradry atmosphere filled glovebox with less than 0.2 ppm water (in volume) was employed for the fabrication including chemical batching, glass melting, preform making and annealing.

The compositions of the studied tellurite glasses were $75TeO_2$-$20ZnO$-$5Na_2O$ (TZN), $75TeO_2$-$20ZnO$-$4Na_2O$-$2NaCl$ (TZNX), and $60TeO_2$-$20PbO$-$20PbCl_2$ (TLX) (mol.%). Commercial chemicals, tellurium dioxide (TeO_2), zinc oxide (ZnO), sodium carbonate (Na_2CO_3), sodium chloride (NaCl), lead oxide (PbO), lead chloride ($PbCl_2$), with purity better than 99.999% were used as raw materials for the glass melting. For each composition, a batch of 70-gram powder was well mixed in a plastic bottle and then melted in a gold crucible inside a furnace in the glovebox at 700–900 °C for 2 h.

The melt was then cast in a preheated metal mold, and a bubble-free glass rod with an outer diameter (OD) of 16 mm and length between 45–65 mm was obtained. Figure 2 shows the photograph of the tellurite glass rods with 16 mm outer diameter (OD). A customized soft glass fiber drawing tower was employed for drawing each rod into an unclad fiber with an OD of 180 μm, with the yield >50 m. A bulk sample was then obtained from the preform remainder with two parallel ends polished.

Figure 2. Optical photograph of tellurite glass rods with 16 mm outer diameter (OD): (**a**) $75TeO_2$-$20ZnO$-$4Na_2O$-$2NaCl$ (TZNX). (**b**) $60TeO_2$-$20PbO$-$20PbCl_2$ (TLX).

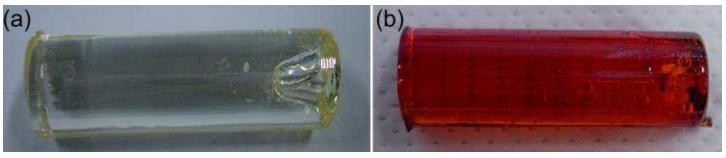

A customized soft-glass fiber drawing tower was used for fiber drawing. A mixed N_2 and O_2 gas with the same moisture level was used as the purge in the furnace on the fiber drawing tower during the fiber drawing.

The transmission spectra of the polished bulk glasses were measured by a Cary 500 Scan UV-VIS-NIR spectrophotometer from 190 to 2500 nm and by a Varian 670-IR FT-IR spectrometer (Fourier transform infrared) spectrophotometer from 2.5 to 25 μm (*i.e.*, 4000–400 cm^{-1}), respectively. The absorption coefficient (in the unit of cm^{-1}) of the residual OH impurity in the bulk glass was calculated according to the Beer-Lambert law and converted to the bulk attenuation in dB/m. After loading the sample, dry N_2 gas was purged into the measurement chamber for at least 5 min to minimize the water vapor and carbon dioxide before the measurement was carried out.

A NICOLET 5700 FT-IR spectrometer (Thermo Electron Corporation) was employed for the loss measurement of the unclad TZNX and TLX fibers in the 1.0–4.8 μm region. The propagation loss of the fiber was measured using the cutback method. The total cutback length for TZNX and TLX unclad fibers was 7 cm and 52 cm respectively.

Another measurement of the OH induced loss in the fabricated dehydrated tellurite fibers was carried out using a crystal OPO based on 1064 nm nanosecond laser pumped magnesium oxide doped periodically lithium niobate (MgO:PPLN) (Covesion Ltd). The idler of the OPO was tuned between 2.8–4.0 μm. The losses of each fiber were then measured at each discrete wavelength with the cutback method. At each wavelength, at least 7 cutback points were measured. The total cutback length for TLX fiber samples was between 50–70 cm, while for TZNX fiber samples it was 25 cm for 3.2–3.6 μm range and 40 cm for other wavelengths.

The refractive index of the TLX glass was measured from 0.3 to 4.0 μm, using Alpha-SE Spectroscopic Ellipsometer (J.A. WOOLLAM CO. INC., Lincoln, NE 68508, USA) between 0.3–1.7 μm and a home-made laser diffractive refractometer at 2.0, 3.0 and 4.0 μm respectively.

The micro-Raman spectra of polished tellurite glass samples were measured using a Renishaw Raman Microscope with a depolarized 632.8 nm HeNe laser source. For each scan, the red laser was focused on the top surface of the sample with the assistance of the CCD camera on the Raman microscope.

3. Results and Discussion

3.1. OH-Induced Attenuation in Dehydrated Tellurite Bulks and Unclad Fiber

Figure 3 shows the OH-induced attenuation of dehydrated tellurite bulk glasses. The polished TZN, TZNX and TLX samples are 4.20, 8.75 and 2.70 mm thick, respectively. It is seen that, for the TZN glass, which was melted in the dry atmosphere with water content of less than 0.2 ppm, the OH-induced loss peaking at 3.4 μm is reduced down to 0.38 cm^{-1}, which is one order of magnitude lower than that in the TZN glass melted in the open atmosphere [16]. This result is close to that reported by Ebendorff-Heidepriem *et al.*, in [18], in which the TZN glass was melted in the dry atmosphere with 10 ppm water content. This can be explained that, during the glass melting, only the surface of the glass melt can be dehydrated by the dry atmosphere and the convection of the melt from the inner body to the surface is fairly slow. In the limited melting time, the amount of the OH impurity in the glass melt is weakly related to the water content in the melting atmosphere. It must be noted that choosing a

very long melting time (e.g., more than 10 h) is not ideal because it will cause significant evaporation from the melt and, consequently, a large deviation of the final glass composition from the designed one.

Figure 3. OH-induced attenuation of dehydrated $75TeO_2$-$20ZnO$-$5Na_2O$ (TZN), $75TeO_2$-$20ZnO$-$4Na_2O$-$2NaCl$ (TZNX) and $60TeO_2$-$20PbO$-$20PbCl_2$ (TLX) bulk glasses.

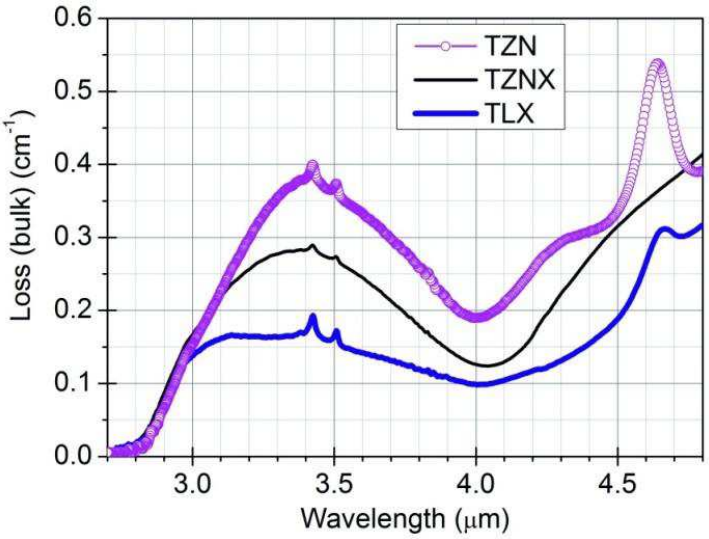

An active approach is therefore necessary for further removing the OH content in the tellurite glass and fiber. It is known that reactive atmosphere processing (RAP) is an effective approach for dehydrating fluoride glasses [19]. Dry reactive halogen gas (such as NF_3, HF, SF_6, and CCl_4) is purged into the fluoride melt to react with the OH groups inside the glass. The hydroxyl groups bonded with the glass network via hydrogen bonding are converted into the volatile compounds HF or HCl, which can be removed from the melt naturally at high temperature. Chlorine drying is also a common method in the fabrication of silica fiber preforms to reduce the OH peaks at 1.38 μm (first overtone) [20]. For tellurite glasses, in order to avoid using highly toxic and reactive halogen gases, halogen-containing solid compounds are preferable. Previously, fluorotellurite glass, obtained by introducing fluorine into the oxide tellurite glass matrix, has been proposed to remove the OH groups with the assistance of fluorine, and also to extend the mid-IR transmission [21]. However, the oxyfluoride glass has strong tendency to be crystallized easily during the heating process and hence is not a thermally stable host material for fiber drawing. Also the introduction of fluorides causes the glass hygroscopic. In addition, introducing fluorides into tellurite glasses, results in significant decrease of both the refractive index and the nonlinear refractive index [21]. In this work we have introduced solid-state chloride compounds, such as NaCl and $PbCl_2$, into the glass composition. Here the chemical reaction between chlorine and OH during the glass melting is a pyrohydrolysis reaction, which can be expressed as $OH^- + Cl^- = HCl\uparrow + O^{2-}$.

As seen in Figure 3, for the TLX glass, it is seen that the OH-induced loss is further reduced down to 0.17 cm^{-1} at 3.4 μm by another factor of 2.2 in comparison with the TZN glass. The addition of NaCl for the TZNX glass did not show a dehydration effect as effective as $PbCl_2$. The solubility of $PbCl_2$ in water is 4.5 g/L (*i.e.*, 1.62×10^{-2} mol/L) at 20 °C and thus practically it is insoluble, while the solubility of NaCl in water is 359 g/L *i.e.*, 6.15 mol/L at 20 °C) [22]. Therefore, NaCl raw chemical can be contaminated by the moisture much more easily than $PbCl_2$. In addition, the molar percentage

of the chlorine in TLX composition is 20 times higher than that in the TZNX composition and it might be another reason responsible for the capability for removing OH impurity from the glass melt. As explained by the above pyrohydrolysis reaction, the chlorides not only replace the OH impurity inside the glass melt, but also generate HCl vapor. The latter is in the bubble state and continuously leaves from the glass melt. It effectively stirs the whole glass melt and lets the whole melt have enough chance to access the interface of the glass melt and the dry atmosphere.

In addition, for all three curves in Figure 3 there are two small peaks at 3.43 µm and 3.51 µm, which are artifacts arising from the protective polymer thin film coated on the optic elements in the VARIAN FTIR instrument.

Figure 4. Comparison of OH-induced attenuation of dehydrated (**a**) TZNX and (**b**) TLX glass unclad fibers (red curve for left axis) and bulks (blue curve for right axis).

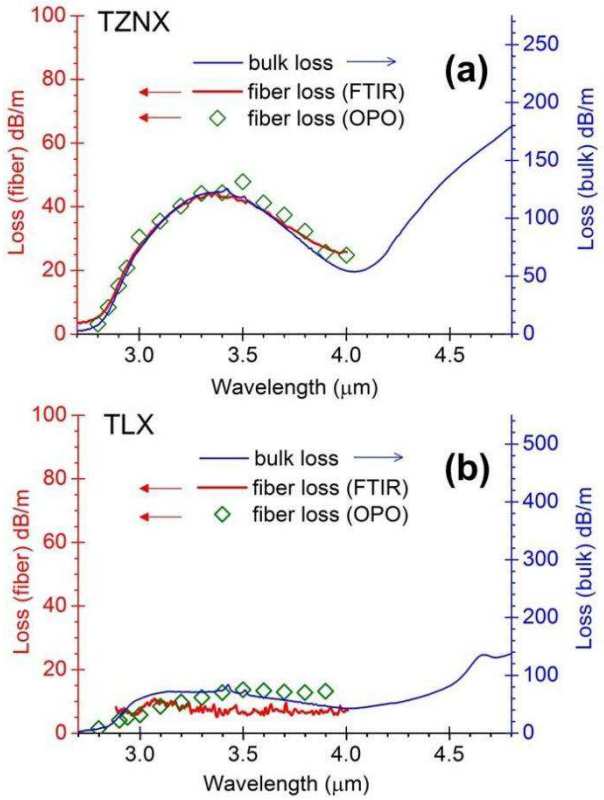

In Figure 4a,b, the red curve for the left axis is the loss curve of the dehydrated unclad fiber; the blue curve for the right axis is the bulk loss of the glass from the same preform. The total cutback length for TZNX and TLX unclad fibers was 7 cm and 52 cm respectively. It is seen that the loss curves of the fiber and bulk match each other fairly well in terms of the lineshape, but for the absolute value, there is a deviation with a factor of 3–7 between the bulk and the fiber. This is mainly because (i) the thickness of the bulk is not sufficiently large to give an accurate loss value when the OH-induced loss is reduced from 1000 dB/m level to 100 dB/m level, and (ii) during the polishing procedure, there might be contamination from the polishing liquid on the bulk surface. On the other hand, these are not issues in the cutback loss measurement for the unclad fibers and the loss measured from the fiber should be reliable.

In order to confirm the validity of the above statement, the losses of the dehydrated TZNX and TLX unclad fibers were also measured at some discrete wavelengths between 2.8–4.0 µm using the MgO: PPLN based OPO. From Figure 4a,b, it is seen that the measured fiber loss values using the OPO are close to the results from the FTIR measurement. For each sample, at the peak wavelength, the absolute difference between the fiber loss using the FTIR method and the one using the OPO is no more than 5 dB/m.

It is worth mentioning that there has been 12 months between the fiber loss measurement from the FTIR and the later one using the OPO source, while the unclad TLX fiber has been stored in the air without any special care. No significant degrading is observed in terms of the loss value.

Therefore, under the dehydration process using halo-tellurite glasses containing lead chloride, the OH-induced loss at 3.4 µm has been reduced down to 10 dB/m, corresponding to OH levels of 1 ppm in weight. Compared with the previously reported lowest OH-induced loss (90–100 dB/m at 3.3 µm) in tellurite glass fibers [18], our results show one order of magnitude improvement.

Additionally, the loss of the TLX unclad fiber was measured to be 0.6 dB/m at 1.55 µm using the cutback method, indicating that the scattering losses due to the defects like bubbles inside the glass fiber should be negligible, because the viscosity of the glass melt was well controlled to avoid the bubbles when the glass rods was made.

3.2. Refractive Index, Dispersion and Nonlinearity of Dehydrated Tellurite Glasses

Figure 5. Refractive index curves of TZN and TLX glasses.

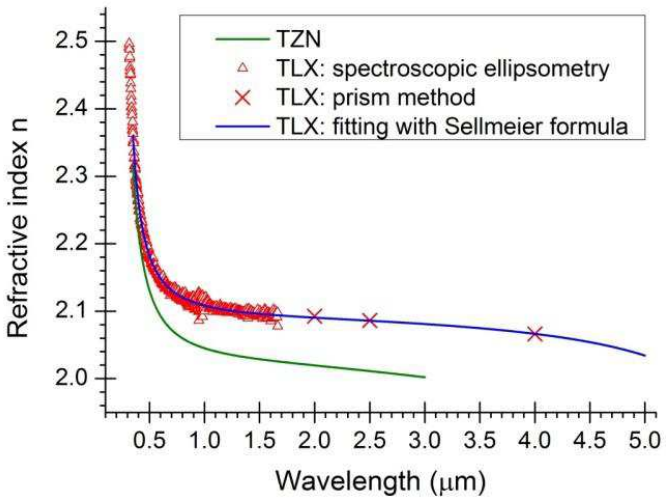

The measured refractive index of TLX glass was fitted using the three-term Sellmeier equation $n^2(\lambda) = 1 + B_1\lambda^2/(\lambda^2 - C_1) + B_2\lambda^2/(\lambda^2 - C_2) + B_3\lambda^2/(\lambda^2 - C_3)$, in which λ is wavelength in micrometers, and B_i (i = 1, 2, 3) and C_i (i = 1, 2, 3) are the coefficients of the equation, for the TLX glass, the fitted six coefficients are seen in Table 2. Figure 5 shows the refractive index and material dispersion curves of TLX glass from 0.3 to 5µm. The refractive index curve of TZN glass was also plotted in Figure 5 in the range of 0.4–3 µm, according to the Sellmeier parameters of similar tellurite glasses [11]. Because the composition of TZN is very close to TZNX, their index and dispersion curves should be very close to each other.

It is seen from Figure 6 that the zero material dispersion wavelength λ_0 of TLX glass is located at 2.30 μm, while λ_0 of TZN glass is located at 2.15 μm. This is useful information for designing dispersion tailed mid-IR nonlinear fiber using the TLX composition in the future.

Figure 6. (**a**) Dispersion curves of TZN and TLX glasses; (**b**) Detailed curves of TZN and TLX near their zero material dispersion wavelengths.

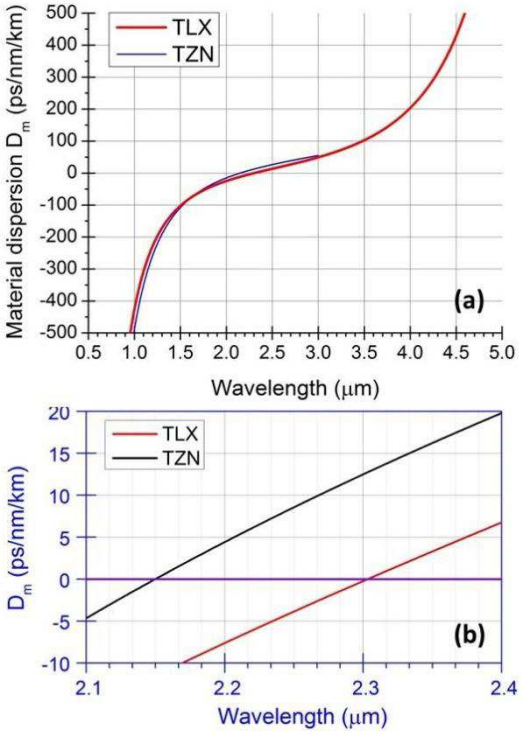

Table 2. Sellmeier coefficients of TLX glass.

Sellmeier coefficients Glass	B_1	C_1	B_2	C_2	B_3	C_3
TLX	1.212	6.068×10^{-2}	2.157	7.068×10^{-4}	0.1891	45.19

Based on the measured refractive index, the nonlinear refractive index n_2 of TLX glass was calculated using the well-known BGO equation [23]:

$$n_2\left(10^{-13}\frac{m^2}{W}\right) = \frac{68 \times (n_d - 1) \cdot (n_d^2 + 2)^2}{2.387 \times 10^6 \cdot n_0 \cdot \nu_d \cdot \left[1.517 + \frac{(n_d^2 + 2) \cdot (n_d - 1) \cdot \nu_d}{6n_d}\right]^{\frac{1}{2}}} \quad (1)$$

where ν_d is the Abbe number ($\nu_d = (n_d - 1)/(n_F - n_C)$, n_d, n_F, and n_C are the refractive indices at 587.6 nm, 486.1 nm and 656.3 nm respectively), and n_0 is the refractive index at the interesting wavelength, respectively. The n_2 of the TLX glass is calculated to be 5.0×10^{-19} m^2/W, about 20 times higher than that of silica glass and also higher than TZN glass (1.7×10^{-19} m^2/W [12]) and the lead silicate glass Schott SF57 (4.1×10^{19} m^2/W [24]).

In addition, it is worth noting that the BGO formula is empirical and there is deviation between the n_2 values calculated by the BGO equation and the values obtained by various measurements [23]. As stated in Reference [23], the agreement between the calculation and the measurement is quite good for

low index, low dispersion materials, but becomes progressively worse for high index, high dispersion materials because the presence of polarizable ions like heavy metals causes the deviation of the dispersion curve from the assumed linear form. However, because the experiment for measuring the n_2 of bulk samples is normally complicated, the BGO equation is still a reliable and convenient tool to estimate the n_2 values of glasses.

Figure 7. Relative reduced Raman intensities of studied tellurite glasses and referenced pure silica glass, normalized to the peak intensity of silica at 440 cm^{-1}.

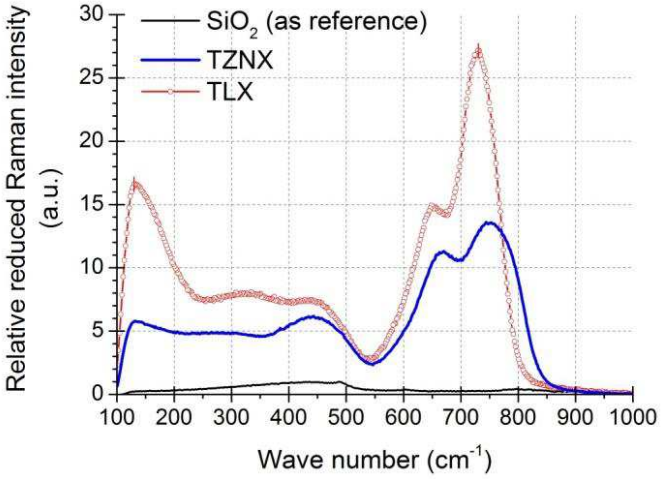

3.3. Raman Gain Coefficients of Dehydrated Tellurite Glasses

Figure 7 shows the calculated relative reduced Raman intensities of the studied tellurite glasses in comparison with a referenced pure silica glass, normalized to the peak intensity of silica at 440 cm^{-1}. The calculation procedure of relative reduced Raman intensity was described in detail in [25] by Shi *et al.* The TLX glass has a calculated peak Raman gain coefficient g_R of 22.6 × 10^{-11} cm/W at 1.55 µm, ~35 times higher than that of silica (0.638 × 10^{-11} cm/W), indicating the potential as a mid-IR fiber-based Raman gain medium.

4. Conclusions

In conclusion, we report a new dehydrated halo-tellurite glass unclad fiber with the lowest recorded OH content (1 ppm in weight) and the lowest OH-induced loss (10 dB/m level) in the 3–4 µm region. The high nonlinear refractive index and the high Raman gain coefficient of the new tellurite glass, indicate the potential for fiber based nonlinear applications in the 2–5 µm region. Currently, work is mainly focused on: (i) further reducing the OH content down to the level 0.1 ppm in weight and the OH-induced loss to 1 dB/m, by optimizing dehydration conditions (e.g., chlorine addition and melting time); and (ii) fabricating fibers with core/cladding structures, including hollow core fiber and small core highly nonlinear fiber for mid-IR applications.

Acknowledgments

This research is partially funded by the Engineering and Physical Sciences Research Council (UK) via the EPSRC Centre for Innovative Manufacture in Photonics and the European Commission—The Seventh Framework Programme—CLARITY project.

Conflicts of Interest

The authors declare no conflict of interest.

References

1. Schliesser, A.; Picqué, N.; Hänsch, T.W. Mid-infrared frequency combs. *Nature Photon.* **2012**, *6*, 440–449.
2. Russell, P.S.J. Photonic crystal fibers. *Science* **2003**, *299*, 358–362.
3. Ranka, J.K.; Windeler, R.S.; Stentz, A.J. Visible continuum generation in air-silica microstructure optical fibers with anomalous dispersion at 800 nm. *Opt. Lett.* **2000**, *25*, 25–27.
4. Serkland, D.K.; Kumar, P. Tunable fiber-optic parametric oscillator. *Opt. Lett.* **1999**, *24*, 92–94.
5. Cundiff, S.T.; Ye, J. Colloquium: Femtosecond optical frequency combs. *Rev. Mod. Phys.* **2003**, *75*, 325–342.
6. Szigeti, B. Polarisability and dielectric constant of ionic crystals. *Trans. Faraday Soc.* **1949**, *45*, 155–166.
7. Boniort, J.Y.; Brehm, C.; DuPont, P.H.; Guignot, D.; Le Sergent, C. Infrared Glass Optical Fibers for 4 and 10 Micron Bands. In Proceedings of the 6th European Conference on Optical Communication, York, UK, 16–19 September 1980; pp. 61–64.
8. Poulain, M.; Poulain, M.; Lucas, J.; Brun, P. Verres fluores au tetrafluorure de zirconium proprietes optiques d'un verre dope au Nd^{3+}. *Mat. Res. Bull.* **1975**, *10*, 243–246, (in French).
9. Kapany, N.S.; Simms, R.J. Recent developments of infrared fiber optics. *Infrared Phys.* **1965**, *5*, 69–75.
10. Wang, J.S.; Vogel, E.M.; Snitzer, E. Tellurite glass: A new candidate for fiber devices. *Opt. Mater.* **1994**, *3*, 187–203.
11. Ghosh, G. Sellmeier coefficients and chromatic dispersions for some tellurite glasses. *J. Am. Ceram. Soc.* **1995**, *78*, 2828–2830.
12. Feng, X.; Loh, W.H.; Flanagan, J.C.; Camerlingo, A.; Dasgupta, S.; Petropoulos, P.; Horak, P.; Frampton, K.E.; White, N.M.; Price, J.H.V.; *et al.* Single-mode tellurite glass holey fiber with extremely large mode area for infrared nonlinear applications. *Opt. Express* **2008**, *16*, 13651–13656.
13. Feng, X.; Flanagan, J.C.; Frampton, K.E.; Petropoulos, P.; White, N.M.; Price, J.H.V.; Loh, W.H.; Rutt, H.N.; Richardson, D.J. Developing single-mode tellurite glass holey fiber for infrared nonlinear applications. *Adv. Sci. Technol.* **2008**, *55*, 108–117.
14. France, P.W.; Carter, S.F.; Williams, J.R.; Beales, K.J.; Parker, J.M. OH-absorption in fluoride glass infra-red fibres. *Electron. Lett.* **1984**, *20*, 607–608.
15. Feng, X.; Tanabe, S.; Hanada, T. Hydroxyl groups in erbium-doped germanotellurite glasses. *J. Non-Crystall. Solids* **2001**, *281*, 48–54.
16. Humbach, O.; Fabian, H.; Grzesik, U.; Haken, U.; Heitmann, W. Analysis of OH absorption bands in synthetic silica. *J. Non-Crystall. Solids* **1996**, *203*, 19–26.

17. Domachuk, P.; Wolchover, N.A.; Cronin-Golomb, M.; Wang, A.; George, A.K.; Cordeiro, C.M.B.; Knight, J.C.; Omenetto, F.G. Over 4000 nm bandwidth of mid-IR supercontinuum generation in sub-centimeter segments of highly nonlinear tellurite PCFs. *Opt. Express* **2008**, *16*, 7161–168.
18. Ebendorff-Heidepriem, H.; Kuan, K.; Oermann, M.R.; Knight, K.; Monro, T.M. Extruded tellurite glass and fibers with low OH content for mid-infrared applications. *Opt. Mater. Express* **2012**, *2*, 432–442.
19. Comyns, A.E. *Fluoride glasses*; Wiley: Hoboken, NJ, USA, 1989; pp. 84–85.
20. Nagel, S.; MacChesney, J.B.; Walker, K. An overview of the modified chemical vapor deposition (MCVD) process and performance. *IEEE Trans. Microwave Theory Tech.* **1982**, *18*, 459–476.
21. O'Donnell, M.D.; Miller, C.A.; Furniss, D.; Tikhomirov, V.K.; Seddon, A.B. Fluorotellurite glasses with improved mid-infrared transmission. *J. Non-Crystall. Solids* **2003**, *331*, 48–57.
22. Brown, T.L.; Lemay, H.E.; Burnsten, B.E. *Chemistry—the Central Science.*, 6th ed.; Prentice Hall: New York, NY, USA, 1994; p. 1017.
23. Boling, N.L.; Glass, A.J.; Owyoung, A. Empirical relationships for predicting non-linear refractive-index changes in optical solids. *IEEE J. Quantum Electron*. **1978**, *QE-14*, 601–608.
24. Kiang, K.M.; Frampton, K.; Monro, T.M.; Moore, R.; Tucknott, J.; Hewak, D.W.; Richardson, D.J.; Rutt, H.N. Extruded single-mode non-silica glass holey optical fibres. *Electron. Lett.* **2002**, *38*, 546–547.
25. Shi, J.; Feng, X.; Horak, P.; Chen, K.K.; Teh, P.S.; Alam, S.-U.; Loh, W.H.; Richardson, D.J.; Ibsen, M. 1.06 μm picosecond pulsed, normal dispersion pumping for generating efficient broadband infrared supercontinuum in meter-length single-mode tellurite holey fiber with high Raman gain coefficient. *J. Lightwave Technol.* **2011**, *29*, 3461–3469.